17th World Conference on Nondestructive Testing, 25-28 Oct 2008, Shanghai, China

Quality assessment of welded joints by the metal magnetic memory method compared to conventional NDT methods and means for materials' properties assessment.

Anatoly DUBOV, Sergey KOLOKOLNIKOV

Energodiagnostika Co. Ltd.

Office 12, Yubileiny prospect, 8, Reutov, Moscow region 143965, Russia

Tel:+7-495-723-83-22 Fax: +7-498-661-61-35

E-mail: mail@energodiagnostika.ru Web:http://www.energodiagnostika.com

Abstract:

A principally new method of products and welded joints metal diagnostics, based on the use of metal magnetic memory (MMM) effect, is developed and successfully implemented in various industries of Russia and other countries nowadays.

The MMM method – is a non-destructive testing method based on distribution analysis of self-magnetic leakage field (SMLF) naturally formed during welding and operation.

SMLF reading provides a unique possibility to integrally assess in the quick testing mode the actual weld state taking into account structural inhomogeneity and distribution of residual stresses and welding defects. At that no weld metal surface preparation is required.

Criteria of power engineering welded joints assessment based on MMM-inspection results are presented. Results of different dimension-type pipeline welded joints comparative inspection by the MMM method and conventional NDT methods (radiography, ultrasonic testing) are given.

Key words: metal magnetic memory, NDT, residual stress, self-magnetic leakage field

1. Introduction.

One of the important and complex problems of modern non-destructive testing (NDT) of various-type welded joints quality is search and detection of their "weak link" in a uniform complex system of factors "structural-mechanical inhomogeneity – weld defects – structural and process stress concentrator", i.e. of zones with high stress-strained state inhomogeneity or stress concentration zones (SCZs). This is important both at welded joints production, i.e. directly after welding, for technological process optimization and at their operation.

Welding exists in the world for more than 100 years, and the most important factor determining reliability of a welded joint – distribution of residual welding stresses – is not still evaluated due to the lack of NDT methods suitable for wide practical application.

Conventional flaw detection oriented only to searching of discontinuity flaws in welded joints

cannot ensure authentic assessment of their quality. It is difficult for a welding technologist to reveal the reasons for weld defectiveness and to improve welding technique based on flaw detection results only.

In conditions when welded joints reliability is affected by many factors, a NDT method, which would integrally assess welded joint metal state, is required.

A principally new method of products and welded joints metal diagnostics, based on the use of metal magnetic memory (MMM) effect, is developed and successfully implemented in various industries of Russia and other countries nowadays.

According to ISO 24497-1:2007 (E) [1] the **metal magnetic memory (MMM)** is an after-effect which occurs as residual magnetization in components and welded joints formed in the course of their fabrication and cooled down to ambient temperatures under interaction with weak magnetic fields or due to irreversible change of the local magnetization state of components in zones of stress concentration and damage under working.

The **method of metal magnetic memory (MMM method)** is a non-destructive testing method based on the analysis of SMLF distribution on components' surfaces for determination of stress concentration zones, imperfections, and heterogeneity in the microstructure of the material and in welded joints.

Self-magnetic-leakage field of the components (SMLF) is a magnetic-leakage field occurring on the component's surface in the zones of stable slip bands of dislocations under operational or residual stresses or in the zones of strong heterogeneity in the microstructure of the material. Papers [2, 3, 4, 5] describe in more detail basic physics and practical capabilities of the MMM method.

Reading SMLF, reflecting residual magnetization naturally formed during welding, provides a unique possibility to integrally assess the actual weld state taking into account structural inhomogeneity and distribution of residual stresses and welding defects.

All defects (discontinuity flaws), occurring in welded joints at the stage of their production, are stress concentrators. However, not all of them will develop in the course of operation, as the mechanical energy density in a stress concentration zone may be insufficient to ensure development of a defect. Basic task of the MMM method is determination of defects parameters at simultaneous assessment of their stressed state.

At present a sufficient experience in welded joints inspection is accumulated and a methodology for magnetic signals decoding is available, when defect length and depth can be determined by signal amplitude and width. The MMM method application in the field of flaw detection actively develops nowadays. And the MMM method combination with ultrasonic testing (UT), radiographic inspection (RT) or eddy-current testing (EC) is most effective. The

most probable defected zones are preliminarily detected by the MMM method in the quick control mode, and then parameters of defects are clarified using the UT or RT.

MMM-inspection is carried out without metal dressing and special magnetization. It allows performing quick testing of welded joints quality in manual and automatic modes and at mass production on various products of carbon, austenite and ferrite-austenite steel grades [6].

Inspection is carried out using specialized small-sized TSC (magnetometric Testers of Stress Concentration) type instruments with self-contained power supply equipped with scanning and recording devices [7].

Fig.1 shows location of a multi-channel scanning device (SD) on a pipe butt-welded joint at inspection by the MMM method. As it is seen in fig.1, flux-gate transducers *1* and *3* measuring the normal component of the H_p magnetic field are located during inspection opposite heat-affected zone (HAZ) on both weld sides, transducer *2* is located in the middle between them and transducer *4,* turned in the opposite direction, is used for offsetting from the external magnetic field.

Depending on the weld or scanning device width, inspection can be carried out when flux-gate transducers are installed only opposite the weld boundaries.

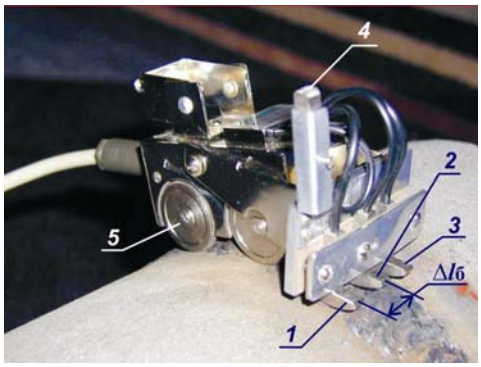

Figure 1. Scheme of pipes butt-welded joints inspection with a multi-channel scanning device of a TSC-type instrument: 1, 2, 3 – flux-gate transducers of the scanning device for the H_p field registration on the weld surface; 4 – flux-gate transducer for offsetting from the external magnetic field; 5 – length meter drive wheels; Δl_b – base distance between flux-gate transducers.

2. Investigation results.

2.1. Detection of surface defects of welds.

Fig.2 shows MMM-inspection results of a R-701/2[1] PVC polymerization chemical reactor bottom radial weld segment. The weld width is 15 mm. The flux-gate transducers of channels

[1] Chemical reactors of the R-701 type were inspected at "Anwil" S.A. (Vlotslavek, Poland). The reactor casing walls are made of 21 mm thick carbon steel. The internal reactor surface on the inspection side was clad with 3 mm thick corrosion-resistant stainless steel 316L (AISI standard (USA)). The width of internal welds of shells was 15 mm.

H_1 and H_2 at MMM-inspection were located opposite to the weld boundaries with HAZ on both weld sides.

Inspection resulted in detection of a SCZ, in which different-polarity H_p field distribution by channels H_1 and H_2 with the maximum field gradients by length (dH/dx) and by base (dH/dz) was recorded. In the inspection scheme (fig.1) the base distance Δl_b between the measurement channels in this case corresponds to the distance Δz between channels H_1 and H_2 or at the software processing – to dH/dz.

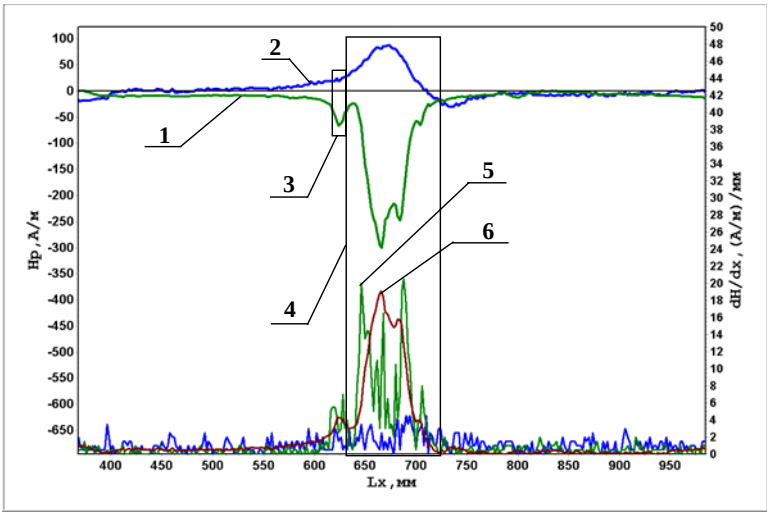

Figure 2. Inspection results of a R-701/1 chemical reactor bottom radial weld: 1 – graph of the H_p field distribution of channel H_1; 2 – graph of the H_p field distribution of channel H_2; 3 – segment with a longitudinal surface crack L=15 mm; 4 – SCZ; 5 – graph of the field gradient dH/dx distribution of channel H_1; 6 – graph of the field gradient dH/dz distribution between channels H_1 and H_2.

Eddy-current inspection (EC) detected a 15 mm long (L=15 mm) surface longitudinal crack in the SCZ, which was located along the weld boundary (the near-weld zone). Fig.3 shows the scheme of the detected crack location.

It is seen in the magnetogram (fig.2) that section *4* with a SCZ is a continuation of the cracked segment. Fig.3 shows that the zero-value line of the normal component of the field H_p=0 (according to the technique this line corresponds to the SC line) is a continuation of the detected crack. At that, upon carrying out measurements of the H_p field intensity at an equal distance from the line H_p=0, different intensity of the H_p field variation was detected. On the one side of the crack (on the side of the SCZ) at intersection with the line H_p=0 the H_p field varied from -505 A/m to +90 A/m, and on the other side – from -8 A/m to +5A/m. Such pattern of the field gradient variation distribution along and across the weld is visually reflected by the graphs of the gradient dH/dx and dH/dz.

Conclusion about the developing crack mode towards the SCZ was made based on this inspection.

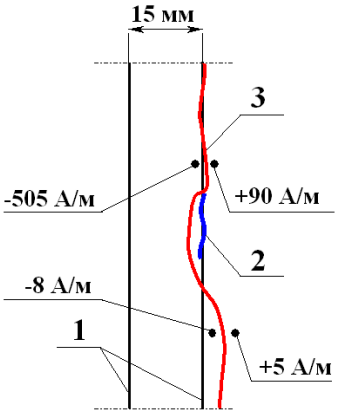

Figure 3. Location of the crack and the H_p=0 line on the radial weld of the R-701/1 chemical reactor bottom: 1 – boundaries of the radial weld of the chemical reactor bottom; 2 – longitudinal crack along the weld boundary; 3 – H_p=0 line.

Fig.4 shows the MMM-inspection results of a steam pipeline (∅325×38mm and ∅219×25mm)

T-welded joint made of steel 15Cr1MoV.

Fig.4, *b* shows a SCZ registered along the weld and characterized by abrupt sign alternation of the H_p field and its gradient *dH/dx* (the graph shows only the first measurement channel H_1).

At additional eddy-current inspection and visually upon metal grinding a longitudinal transverse 20mm long crack, developing on the external ∅219×25 pipe surface perpendicular to the weld, was detected in the SCZ. The maximum variation of the field and its gradient was revealed along channel H_1 located in weld HAZ on the ∅219×25 pipe side (see fig.4, *b*).

Fig.5 shows the results of a T-17[2] heat exchanger weld segment inspection.

In the magnetogram of fig.5,*a* 800 mm long SCZ (*1*) is marked, on which an abrupt multiple amplitude variation of the H_p field with sign alternation along all measurement channels was registered. A transverse 5 mm long crack coming out to the exterior surface (see fig.5, *b*) was detected in the zone of the maximum value of gradient *dH/dx* (*2*) along the measurement channels H_2.

[2] The T-17 heat exchanger casing was put in operation at the "Slavneft-YANOS" enterprise in 1965. The material of the casing is correspond to M 1017 (AISI). The wall thickness is 12 mm. Inspection was carried out in 2003.

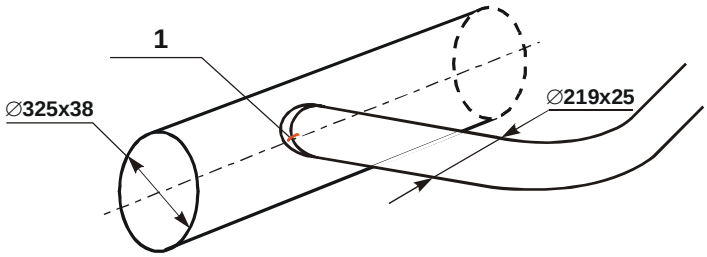

a)

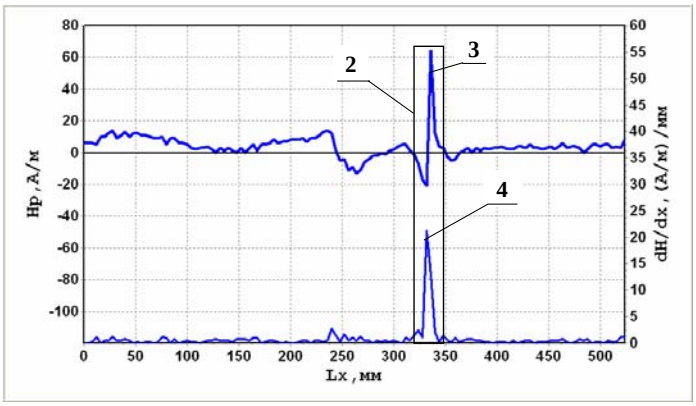

b)

Figure 4. Results of a steam pipeline (∅325×38mm and ∅219×25mm) T-welded joint inspection: a – cracked T-welded joint; b – H_p field and its gradient dH/dx distribution in the SCZ; 1 – crack (L=20mm); 2 – SCZ with a transverse surface crack L=20 mm; 3 – graph of the H_p field distribution of channel H_1; 4 – graph of the field gradient dH/dx distribution of channel H_1.

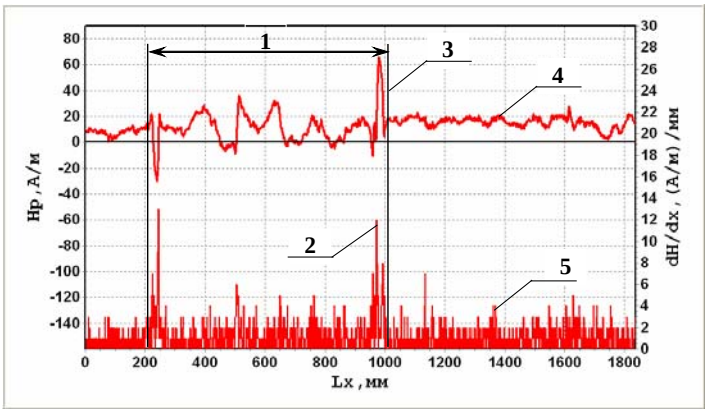

a)

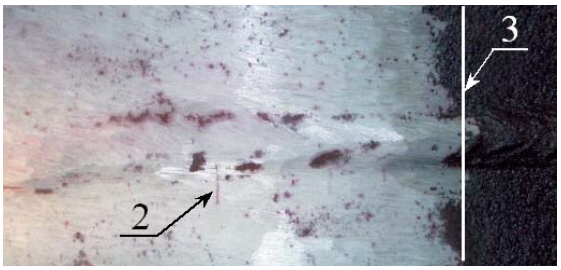

b)

Figure 5. Results of a T-17 heat exchanger weld segment inspection: a – magnetogram of the H_p field and its gradient dH/dx distribution on the weld segment; b – appearance of the defected segment of the weld:

1 – heat exchanger weld segment with a SCZ, specified for dressing for additional inspection;
2 – transverse crack location in the SCZ;
3 – dressed area boundary of the weld segment;
4 – H_p field distribution; 5 – field gradient dH/dx distribution.

Metal polishing with its subsequent etching was carried out in the detected external crack zone upon surface machining. It allowed in the course of metallographic investigation to detect surface damaging of metal in the form of laminations with developing in-depth cracks (see fig.6).

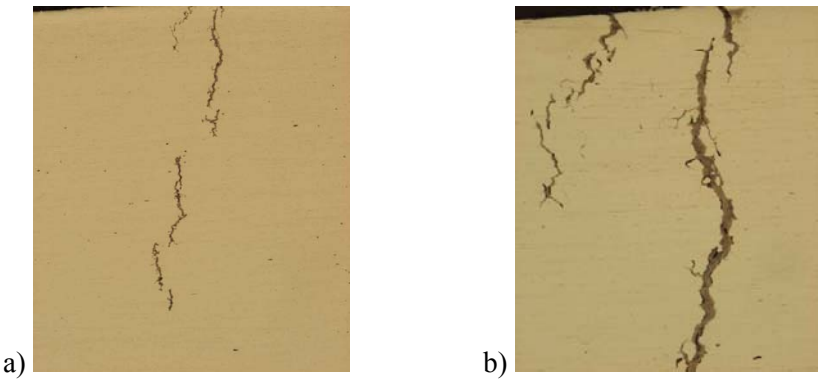

Figure 6. Laminations turning into cracks: a – magnification x50; b – magnification x200.

2.2. Detection of subsurface defects of welds.

Fig.7 shows the fragment of inspection results of the R-701/2 RVC polymerization reactor weld.

It is seen in fig.7, *a* that the total length of the SCZ area is 40 mm. However the length of the segment, on which the field gradient *dH/dx* had the maximum value (*3*) and which corresponded to location of the internal local defect, detected by UT, made 10 mm. Fig.7, *b* shows the diagram of the UT echo-signal from the defect detected at the weld depth of 7,5 mm. UT was carried out with the frequency of 5 MHz using the direct piezoelectric transducer (PET).

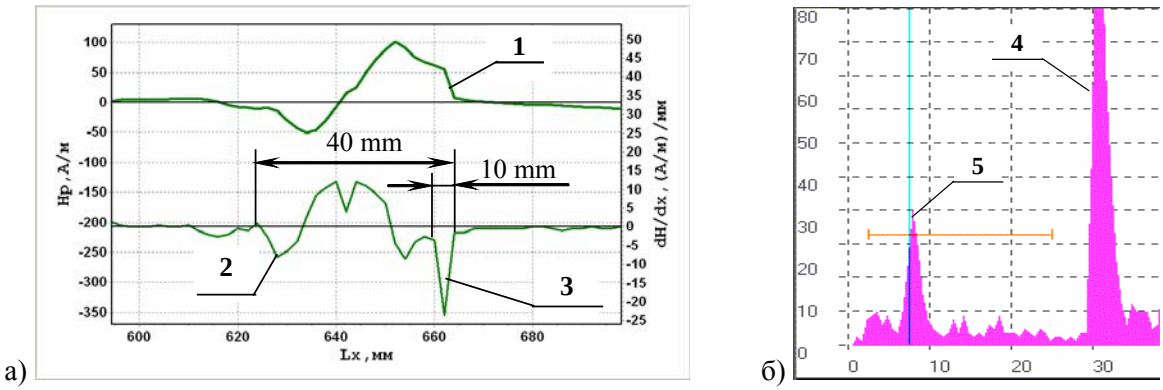

Figure 7. Results of a chemical reactor girth weld segment inspection by the MMM method (a) and UT (b): 1 – graph of the H_p field distribution along the third measurement channel H_3; 2 – graphs of the field gradient dH/dx distribution of channel H_3; 3 – segment with the maximum field gradient corresponding to the defect location at the depth of 7,5 mm; 4 – bottom signal; 5 – signal from the defect located at the depth of 7,5 mm.

Fig.8 presents a circular (hour) magnetogram of field gradients *dH/dx* and *dH/dz* distribution along the girth weld 19-20 of a ∅720×7 mm gas pipeline. Weld segments with local surges of field gradients values corresponded to radiographically confirmed weld defects. Fig.9÷11 show for the sake of comparison fragments of the H_p field and the field gradients *dH/dx* and *dH/dz* distribution on segments of the weld 19-20 in individual SCZs (I, II, III) detected by the MMM method as well as the results of radiographic inspection in these SCZs. Defects screening was performed according to Russian building and assembly norms VSN 012-88 (Part I) for trunk pipelines.

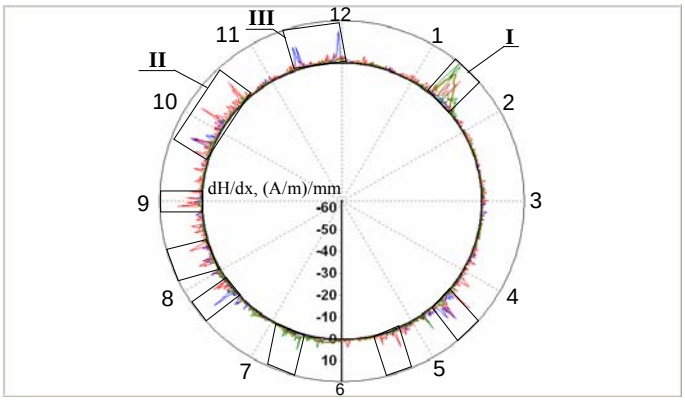

Figure 8. Circle magnetogram of the magnetic field gradients dH/dx and dH/dz distribution along the field welded joint #19-20 of the ∅720x7 mm trunk gas pipeline: ⬚ – location of SCZs detected by the MMM method; 1÷12 – hour scanning.

a)

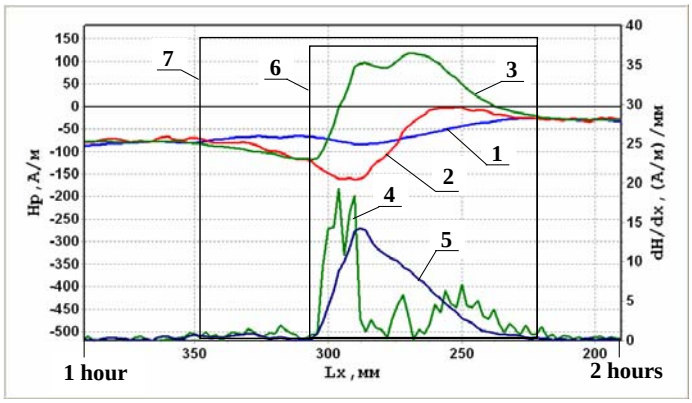

b)

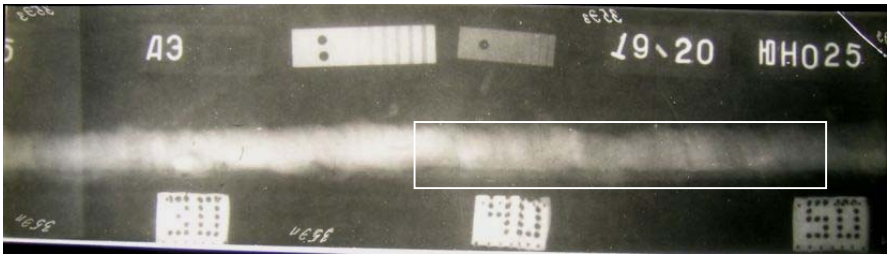

Figure 9. Results of the field girth welded joint #19-20 inspection in SCZ-I (on the 1÷2 hours segment) by the MMM method (a) and radiography (b): 1 – H_p field gradient distribution of channel H_1; 2 – H_p field gradient distribution of channel H_2; 3 – H_p field gradient distribution of channel H_3; 4 – field gradient dH/dx distribution of channel H_3; 5 – field gradient dH/dz distribution between channels H_2 and H_3; 6 – SCZ-I with maximum values of gradients dH/dx and dH/dz (L=75 mm); 7 – segment with visible weld undercut (L=129 mm).

a)

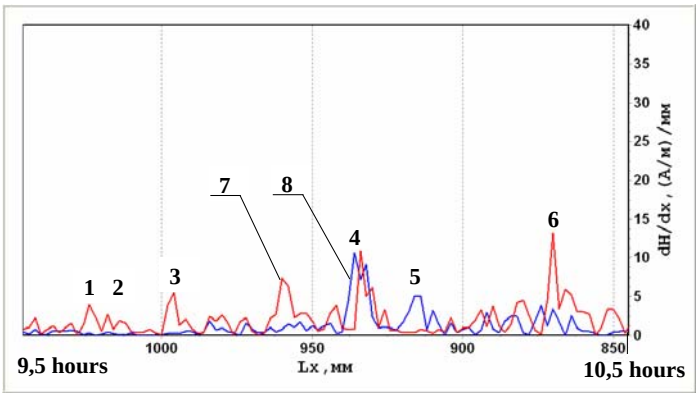

b)

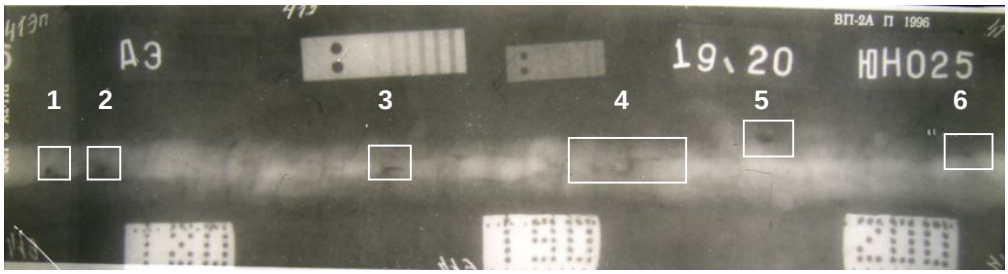

Figure 10. Results of the field girth welded joint #19-20 inspection in SCZ-II (on the 9,5÷10,5 hours segment) by the MMM method (a) and radiography (b): 1 – 1,5mm diameter pore; 2 – 2,5mm diameter pore; 3 – poor penetration of the root L=7mm; 4 – poor penetration between the beads L=25mm; 5 – elongated pore, the length is L=6mm, and poor penetration along the grooving L=10mm; 6 – poor penetration along the grooving L=5mm; 7 – field gradient dH/dx distribution of channel H_2; 8 – field gradient dH/dx distribution of channel H_1.

a)

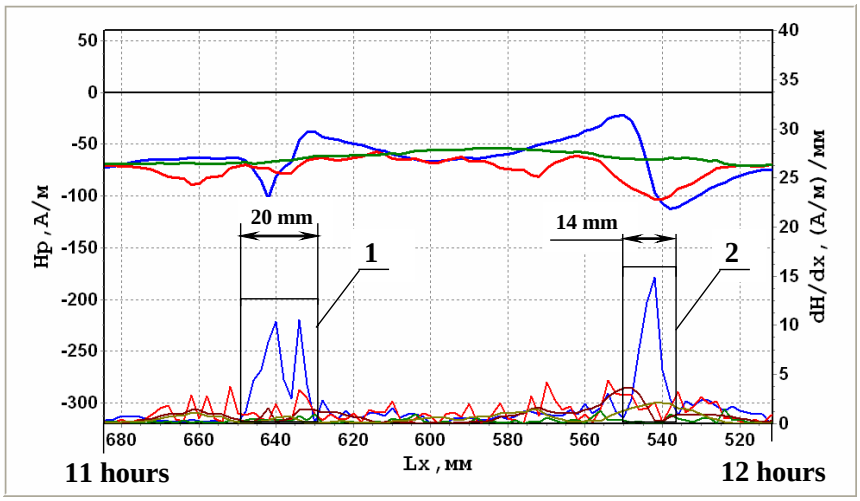

b)

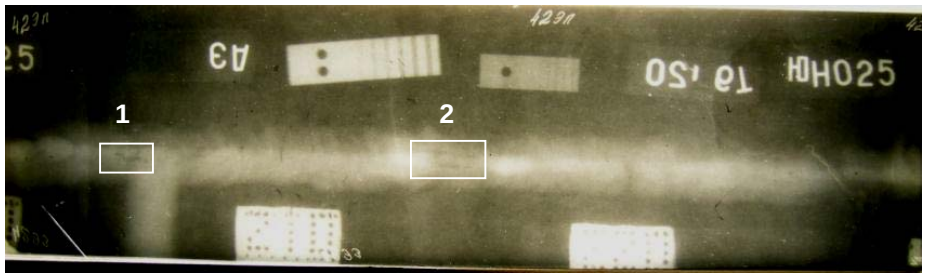

Figure 11. Results of the field girth welded joint #19-20 inspection in SCZ-III (on the 11÷12 hours segment) by the MMM method (a) and radiography (b):
1 – poor penetration of the root, L =10mm (Da10>0,1S);
2 – poor penetration along the weld grooving, L =15mm (Dc10>0,1S).

The circle (hour) magnetogram of fig.12, *a* shows the distribution of the field gradient *dH/dx* along the girth weld perimeter of a ∅720x7mm gas pipeline. Inspection was carried out according to the scheme indicated in fig.1. Fig.12, *b* shows the fragment of the field gradient *dH/dx* distribution in the defected SCZ *A* along one measurement channel going along the weld center. The signal width, corresponding to the defect length according to the MMM method, was 12mm. Based on the data of this weld radiography, an inadmissible defect of the *Da10>0,1S* type – poor penetration in the weld root of not less than 10 mm long was detected in the defected SCZ *A*.

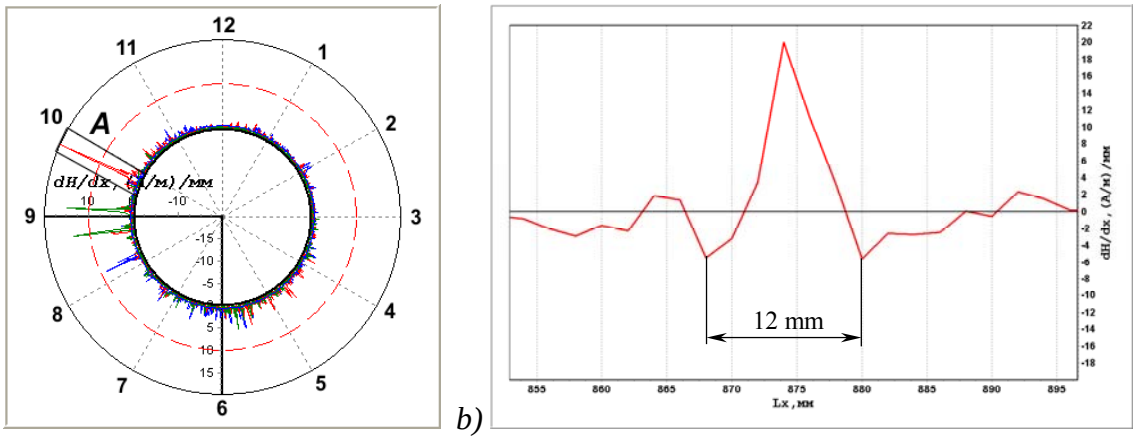

Figure 12. Inspection results of the "turning" girth welded joint #12-13 of the ∅720x7 mm gas pipeline: a – circle magnetogram of the magnetic field gradient dH/dx distribution; b – fragment of the field gradient dH/dx distribution in the defected SCZ A.

Multiple laboratory and industrial investigations revealed the location displacement along the hour scanning of magnetic signals, registered on the weld surface, from the deep-seated defect recorded by RT or UT. Such displacement is determined by the fact that the magnetic signal in the MMM method corresponds to glide planes displaced from the sharp edge of the defect along the weld depth approximately by 45° relative to the maximum stress concentration. Long-range stress fields form long-range domain boundaries along glide planes with exposure to the weld surface in the form of local variations of the magnetic field and its gradient [2, 3].

Approximate calculation of the defected zone burial depth *h* by the MMM method is carried out using trigonometric dependencies according to the scheme shown in fig.13:

$$h = \frac{1}{2}\ell,$$

where ℓ – is the defect length determined by the field gradient graph.

According to the example presented in fig.12 (SCZ *A*) the defect burial depth *h* will make:

$$h = \frac{12mm}{2} = 6mm.$$

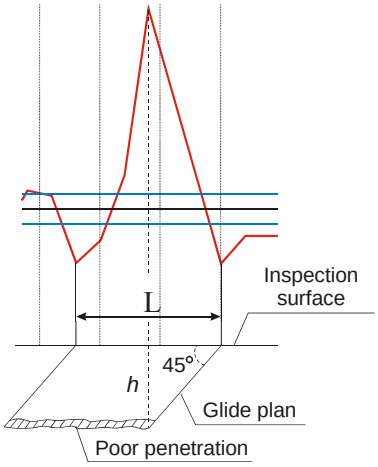

Figure 13. Scheme of a defect burial depth determination by the MMM method.

Based on the performed calculation a conclusion may be drawn about good agreement of inspection results by the MMM method and RT As it was indicated above, according to RT data, the 10 mm long poor penetration was detected in the weld root in zone 1 at the depth of 6÷7 mm.

In case of a long defect in the form of poor penetration in the weld root or grooving, the MMM method registers sign-alternating signals of the field gradient *dH/dx* on the weld surface. Fig.14 shows field gradient distribution in the area of poor penetration along grooving of the field butt-welded joint #12 of a ∅720×7mm trunk gas pipeline. According to the MMM method, the defected segment length in this weld was 124 mm. According to RT data of this weld, the length of poor penetration along the weld grooving was 130 mm. In this example a large number of magnetic signals with sign-alternating nature from long poor penetration, according to the scheme presented in fig.13, is determined by the corresponding number of glide planes occurring in stress concentration zones on defected zone edges. Owing to the magnetomechanical effect, magnetization domains form along these glide planes, and thus the information is transferred to the weld surface.

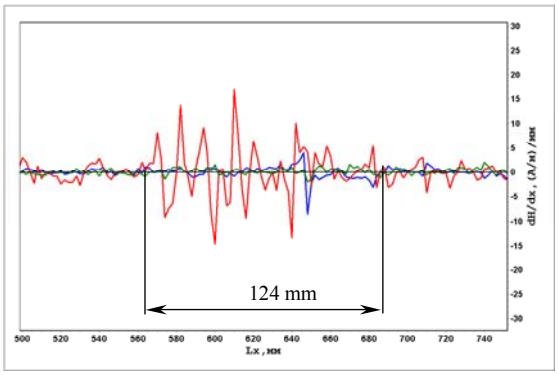

Figure 14. H_p field distribution in poor penetration zone along grooving of field girth butt-welded joint #12 of a ∅720×7 mm trunk gas pipeline.

3. Conclusions.

Based on the results of complex inspection of the same welded joints by the MMM method, radiography and UT the following conclusions were made:

1. At MMM-inspection of welded joints the post descriptive parameters is the normal component of the H_p magnetic field and its gradients along the measurement channel *dH/dx* and by the base between the adjacent measurement channels *dH/dz.* Measurement channels located along the weld boundaries (the near-weld zone) effectively react to long defects like poor fusion, displacement of edges, undercuts and longitudinal cracks. The measurement channel, located along the weld center, effectively reacts to defects in the form of pores and slag inclusions.

2. Segments with weld defects are characterized by anomalous variation of the H_p field with the field gradient value exceeding by two or more times the average gradient level on the weld.

3. Complex welded joints inspection by various NDT methods revealed the high agreement level of inspection results obtained by the MMM method, RT and UT. Unlike UT and RT, the MMM method provides information about the level of stress concentration on the detected defects, i.e. it allows carrying out defects classification by developing and non-developing defects.

4. The practical experience of welded joints NDT demonstrated that inadmissible according to the norms (RT or UT) defects, formed at fabrication but which are free from stress concentration, do not develop in the course of long-term operation. For example, welded joints inspection on trunk gas pipelines being in operation for 30 and more years detected many times inadmissible defects formed as far back as during fabrication.

5. Visualization and documenting of defects on magnetograms in the MMM method has practical advantage as compared to X-ray films at radiographic inspection.

6. Taking into account high agreement of inspection results obtained by the MMM method, radiography and UT, it is appropriate to further apply complex inspection. In the system of steel objects' welds non-destructive testing the MMM method will be maximally effective at the following order of its application:

a) SCZs (defected zones) detection by the MMM method in the quick control mode without any preparation of the weld metal surface.

b) Defects sizes and types (length, burial depth) determination in SCZs by conventional methods (UT, RT – deep-seated defects, EC – detection of surface defects (cracks)).

Reference.

1. ISO 24497-1:2007(E) Non-destructive testing-Metal magnetic memory-Part 1: Vocabulary.

2. A.A. Dubov. Diagnostics of boiler tubes using the metal magnetic memory. Moscow: Energoatomizdat, 1995. 112 p.

3. V.T. Vlasov, A.A. Dubov. Physical bases of the metal magnetic memory method. Moscow: ZAO "Tisso", 2004. 424 p.

4. A.A. Dubov, Al.A. Dubov, S.M. Kolokolnikov. The metal magnetic memory method and inspection instruments. Training handbook" IIW Document No. V-1347.

5. A.A. Dubov. Method of service durability determination of pipes made of ferromagnetic materials. Author's Certificate 1769105. Patent of Russia // BI, No.38. 1992.

6. ISO 24497-2:2007(E) Non-destructive testing-Metal magnetic memory-Part 2: General requirements.

7. ISO 24497-3:2007 (E) Non-Destructive testing – Metal magnetic memory – Part 3: Inspection of welded joints.

8. A.V. Ustinov, A.A. Zhokhov, V.A. Kuzmenko. The metal magnetic memory method application at "Slavneft-YANOS" JSC. Equipment and structures diagnostics using the magnetic memory of metal // Proceeding of Fourth International Scientific and Technical Conference "Diagnostics of equipment and structures using the metal magnetic memory". Moscow: Energodiagnostika Co. Ltd., 2007. 232 p.